

<https://helda.helsinki.fi>

---

## Combined high-power ultrasound and high-pressure homogenization nanoemulsification: The effect of energy density, oil content and emulsifier type and content

Calligaris, Sonia

2018-05

---

Calligaris , S , Plazzotta , S , Valoppi , F & Anese , M 2018 , ' Combined high-power ultrasound and high-pressure homogenization nanoemulsification: The effect of energy density, oil content and emulsifier type and content ' , Food Research International , vol. 107 , pp. 700-707 . <https://doi.org/10.1016/j.foodres.2018.03.017>

---

<http://hdl.handle.net/10138/299853>

<https://doi.org/10.1016/j.foodres.2018.03.017>

---

cc\_by\_nc\_nd

acceptedVersion

---

*Downloaded from Helda, University of Helsinki institutional repository.*

*This is an electronic reprint of the original article.*

*This reprint may differ from the original in pagination and typographic detail.*

*Please cite the original version.*

## Accepted Manuscript

Combined high-power ultrasound and high-pressure homogenization nanoemulsification: The effect of energy density, oil content and emulsifier type and content

Sonia Calligaris, Stella Plazzotta, Fabio Valoppi, Monica Anese

PII: S0963-9969(18)30184-4  
DOI: doi:[10.1016/j.foodres.2018.03.017](https://doi.org/10.1016/j.foodres.2018.03.017)  
Reference: FRIN 7454

To appear in: *Food Research International*

Received date: 20 November 2017

Revised date: 1 March 2018

Accepted date: 4 March 2018

Please cite this article as: Sonia Calligaris, Stella Plazzotta, Fabio Valoppi, Monica Anese , Combined high-power ultrasound and high-pressure homogenization nanoemulsification: The effect of energy density, oil content and emulsifier type and content. The address for the corresponding author was captured as affiliation for all authors. Please check if appropriate. Frin(2017), doi:[10.1016/j.foodres.2018.03.017](https://doi.org/10.1016/j.foodres.2018.03.017)

This is a PDF file of an unedited manuscript that has been accepted for publication. As a service to our customers we are providing this early version of the manuscript. The manuscript will undergo copyediting, typesetting, and review of the resulting proof before it is published in its final form. Please note that during the production process errors may be discovered which could affect the content, and all legal disclaimers that apply to the journal pertain.



**Combined high-power ultrasound and high-pressure homogenization nanoemulsification: the effect of energy density, oil content and emulsifier type and content**

**Sonia Calligaris\*, Stella Plazzotta, Fabio Valoppi, Monica Anese**

<sup>1</sup>Dipartimento di Scienze AgroAlimentari, Ambientali e Animali, Università di Udine, Udine, Italy

<sup>2</sup>Department of Food and Environmental Sciences, University of Helsinki, Helsinki, Finland

\* Corresponding author. E-mail address: sonia.calligaris@uniud.it

**Abstract**

Combinations of ultrasound (US) and high-pressure homogenization (HPH) at low-medium energy densities were studied as alternative processes to individual US and HPH to produce Tween 80 and whey protein stabilized nanoemulsions, while reducing the energy input. To this aim, preliminary trials were performed to compare emulsification efficacy of single and combined HPH and US treatments delivering low-medium energy densities. Results highlighted the efficacy of US-HPH combined process in reducing the energy required to produce nanoemulsions stabilized with both Tween 80 and whey protein isolate. Subsequently, the effect of emulsifier content (1-3% w/w), oil amount (10-20% w/w) and energy density (47-175 MJ/m<sup>3</sup>) on emulsion mean particle diameter was evaluated by means of a central composite design. Particles of 140-190 nm were obtained by delivering 175 MJ/m<sup>3</sup> energy density at emulsions containing 3% (w/w) Tween 80 and 10% (w/w) oil. In the case of whey protein isolate stabilized emulsions, a reduced emulsifier amount (1% w/w) and intermediate energy density (120 MJ/m<sup>3</sup>) allowed a minimum droplet size around 220-250 nm to be achieved. Results showed that, in both cases, at least 50% of the energy density should be delivered by HPH to obtain the minimum particle diameter.

*Keywords:* high-power ultrasound, high-pressure homogenization, combined technologies, energy reduction, nanoemulsion, food emulsifiers.

## 1. Introduction

The interest in food grade nanoemulsions has rapidly increased in the last decades, due to their unique physico-chemical properties and possible application as delivery systems of bioactive molecules (Karthik, Ezhilarasi, & Anandharamakrishnan, 2017; Sanguansri & Augustin, 2006). Nanoemulsions are heterogeneous systems consisting of two immiscible liquids, with one phase being dispersed as nanometric droplets with diameter lower than 200 nm (Salvia-Trujillo, Soliva-Fortuny, Rojas-Grau, McClements, & Martin-Belloso, 2017). Formation and stabilization of nanoemulsions depend on the physical-chemical properties of constituents, including oil and aqueous phases and emulsifiers, as well as on the energy density, i.e. the energy input per unit volume transferred to the sample. Energy density, in turn, depends on treatment intensity and duration (Mohd-Setapar, Nian-Yian, Nuraisha, Kamarudin, & Idham, 2013; Schubert & Engel, 2004; Schubert, Ax, & Behrend, 2003; Stang, Schuchmann, & Schubert, 2001; Wooster, Golding, & Sanguansri, 2008). Smaller droplets are usually obtained by increasing the emulsifier content and the supplied energy density. Also, at comparable energy densities, the modality of energy delivering can affect the nanoemulsion particle size and stability (Calligaris et al., 2016; Jafari, Assadpoor, He, & Bhandari, 2008). Different mechanical devices capable of generating intense disruptive forces can be used to obtain nanoemulsions. High-power ultrasound (US) and high-pressure homogenization (HPH) are high-energy nanoemulsification processes, which are able to reduce the emulsion particle diameter at nano-level (Abbas, Hayat, Karangwa, Bashari, & Zhang, 2013; Canselier, Delmas, Wilhelm, & Abismail, 2002; Dumay et al., 2013; McClements, 2005; Silva, Cerqueira, & Vicente, 2012). High-power ultrasonic devices form emulsions with nano-sized droplets through the propagation of low frequency sound waves (20-24 kHz), which cause the formation and violent collapse of cavitation bubbles (Abbas et al., 2013; Leong, Wooster, Kentish, & Ashokkumar, 2009). High-pressure homogenizers break large droplets into smaller ones by a combination of intensive disruptive forces, such as shear stress, cavitation and turbulent flow conditions, suffered by the product during the passage in the homogenization valve (Stang et al., 2001). Both technologies require extremely intense treatments (long times in US and high pressures and/or multiple passes in HPH) to produce emulsions with nano-size droplets (Kentish et al., 2008; McClements & Rao, 2011; Qian & McClements, 2011). This implies the use of specifically designed equipment and relatively high running and maintenance costs, due to elevated energy consumption and frequent replacement of wearing parts. Therefore, the industrial application of US and HPH as high-energy emulsification processes is limited because of their low sustainability. Based on these considerations, the possibility to reduce the energy requirements for nanoemulsification might stir up new interest in large-scale production of nanoemulsions. Recently,

it has been demonstrated that combined US-HPH processes can be effective in reducing the energy demand for nanoemulsion preparation by using a combination of food-grade synthetic surfactants (Tween 80 and Span 80) with well-known excellent performances under high-energy emulsification (Calligaris et al., 2016). In particular, US and HPH provided in combination at low and medium energy density values led to nanoemulsions with particle size and stability comparable to those prepared by using individual US or HPH at high energy densities.

The aim of this work was to investigate further US-HPH nanoemulsification in obtaining nanoemulsions in the presence of food grade emulsifiers. To this purpose, preliminary trials were carried out to evaluate the effectiveness of US-HPH combined processes to obtain nanoemulsions containing Tween 80 or whey proteins as emulsifiers. Then, a three-variable face centred central composite design was used to study the effect of emulsifier content (1-3% w/w), oil amount (10-20% w/w) and energy density (48-175 MJ/m<sup>3</sup>) on emulsion mean particle diameter. Finally, the effect of different US and HPH combinations developing the same energy density was studied to identify the optimal energy share between US and HPH allowing minimum droplet diameter to be obtained during a combined process.

## 2. Materials and methods

### 2.1. Coarse emulsion preparation

The aqueous phase was prepared by mixing an amount allowing to obtain in the final emulsion 1 to 3% (w/w) of Tween 80 (Tween 80®, Sigma Aldrich, Milano, Italy) or whey protein isolate (94.7% protein content; 74.6%  $\beta$ -lactoglobulin, 23.8%  $\alpha$ -lactoglobulin, 1.6% bovine serum albumin; Davisco Food International Inc., Le Seur, Germany) with deionized water. The aqueous phase was stirred at 20 °C for 2 h, until the surfactant was completely dissolved. The coarse emulsion was prepared by mixing the aqueous phase with sunflower oil (10-20% w/w) with a high-speed blender (Polytron, PT 3000, Cinematica, Littau, Swiss) at 8000 rpm for 1 min. The coarse emulsion was immediately subjected to the nanoemulsification processes.

### 2.2. Nanoemulsification processes

#### 2.2.1. High-power ultrasound (US)

An ultrasonic processor (Hieschler Ultrasonics GmbH, mod. UP400S, Teltow, Germany) with a titanium horn tip diameter of 22 mm was used. The instrument operated at constant ultrasound amplitude and frequency of 100  $\mu$ m and 24 kHz, respectively. Aliquots of 150 mL of coarse emulsion were introduced into 250 mL capacity (110 mm height, 60 mm internal diameter) glass vessel. The tip of the sonicator horn was placed in the centre of the solution, with an immersion

depth in the fluid of 50 mm. The ultrasound treatments were performed up to 240 s and the temperature was controlled using a cryostatic cooling system set at 4 °C to dissipate the heat generated during the treatment.

### 2.2.2. *High-pressure homogenization (HPH)*

A continuous lab-scale high-pressure homogenizer (Panda Plus 2000, GEA Niro Soavi, Parma, Italy) supplied with two PS type homogenization valves with a flow rate of 10 L/h was used to treat 150 mL of coarse emulsion. The first valve was the actual homogenization stage and was set at increasing pressure up to 150 MPa. The second valve was set at the constant value of 5 MPa. Additional samples were prepared by subjecting the coarse emulsion to HPH for up to 3 successive passes at 120 MPa. At the exit of the homogenizer, the emulsions were forced into a heat exchanger (GEA Niro Soavi, Parma, Italy) and cooled to room temperature.

### 2.2.3. *Combined US-HPH*

The coarse emulsion (150 mL) was subjected to US followed by HPH. The time between the two treatments did not exceed 30s. US treatments were applied for 20 or 60 s, while homogenization pressure was set at 20, 50, 80 and 100 MPa. Further US-HPH treatments consisting of 20 s + 20 MPa, 22 s + 80 MPa and 60 s + 100 MPa were carried out to provide energy densities of 47, 111 and 175 MJ/m<sup>3</sup> according to a central composite design. Finally, to deliver to the sample energy densities of 145 and 120 MJ/m<sup>3</sup>, the percentage ratio between the energy delivered by US and HPH was progressively changed.

### 2.3. *Temperature measurement*

The sample temperature was measured just before and immediately after (i.e. before the cooling step) HPH process and during US by a copper-constantan thermocouple probe (Ellab, Hillerød, Denmark) connected to a portable data logger (mod. 502A1, Tersid, Milan, Italy).

### 2.4. *Energy density computation*

The energy density, i.e. the energy input per unit volume ( $E_v$ , MJ/m<sup>3</sup>), was computed as described by Bot et al. (2017). In particular, the  $E_v$  transferred from the probe to the sample during ultrasound treatments was calculated by using equation (1) (Raso, Mañas, Pagán, & Sala, 1999):

$$E_v = \frac{mc_p(\partial T / \partial t)}{V} \times t \quad (1)$$

where  $m$  is the sample mass (kg),  $c_p$  is the sample heat capacity (4186 J/(kg K)),  $V$  is the sample volume (cm<sup>3</sup>), and  $t$  (s) is the duration of the ultrasonication time.

The energy density transferred from the valve to the sample during the HPH treatment was determined as described by Stang et al. (2001), according to equation (2):

$$E_v = \Delta P \quad (2)$$

where  $\Delta P$  is the pressure difference operating at the nozzles.

The energy density of multiple passes HPH and combined treatments was calculated as the sum of the energy density values of the corresponding single pass HPH or US plus HPH treatments.

## 2.5. Droplet size

The mean diameter of emulsion droplets was measured by using the dynamic light scattering instrument Zetasizer Nano ZS (Malvern, Milan, Italy). Samples were diluted 1:10 (v/v) with deionised water prior to the analysis to avoid multiple scattering effects. The angle of observation was 173°. Solution refractive index and viscosity were set at 1.333 and 1.0 cP, respectively, corresponding to the values of pure water at 20 °C.

## 2.6. Polynomial equations and statistical analysis

Modelling was aimed at describing the variation of mean particle diameter as a function of the variables of the central composite design. In particular, a 3-factors face centred central composite design (CCF) was used. The three considered factors were oil content, emulsifier concentration and energy density. The ranges of variables were chosen on the basis of information from the preliminary trials, showing that the application of values outside the considered intervals led to non-emulsified samples. For each factor, extreme, lower and upper values were identified and combined to form the factorial part of the design (8 factorial points). In particular, oil content, emulsifier concentration and energy density were set at 10, 15 and 20% (w/w), 1, 2 and 3% (w/w) and 48, 111 and 175 MJ/m<sup>3</sup>, respectively. The energy density values were obtained by US-HPH combined treatments of 20 s+20 MPa, 22 s+80 MPa and 60 s+100 MPa. To complete the CCF, 6 axial points (combinations of the extreme value of one factor and the intermediate level for the others) and 1 central point (combination of the intermediate values of the three factors) were defined. All the factorial and axial points were replicated once, while the central point was replicated 6 times. The full set of sampling points is reported in Table 1. A software package (Statistica for Windows v. 10, StatSoft, Inc.) was used to fit the second order response surface to the observed data according to the following equation:



$$y = B_0 + \sum_{i=1}^k B_i x_i + \sum_{i=1}^k B_{ii} x_i^2 + \sum_{j>i \geq 1}^k B_{ij} x_i x_j \quad (3)$$

where  $B_0$  is a constant, and  $B_i$ ,  $B_{ii}$ ,  $B_{ij}$  are regression coefficients of the model,  $x_i$  and  $x_j$  are the independent variables in coded values, and  $k$  is the number of factors.

Shapiro-Wilk test was used to evaluate normality of the data, while the possible presence of outliers and the homogeneity of variance were evaluated by residual analysis. Goodness of fit was measured with the adjusted determination coefficient ( $R^2_{adj}$ ).  $p$ -Values for the coefficients of the response surface were defined using standard  $t$ -test. Three-dimensional counter plots were drawn to illustrate the effects of the considered factors on the responses. To this purpose, the values of the response were plotted on the  $z$ -axis against the two most relevant factors, keeping the third one fixed to a constant value (the central one).

Results relevant to preliminary trials are the average of at least three measurements carried out on two replicated experiments. Data are reported as mean value  $\pm$  standard deviation. Statistical analysis was performed by using R v. 2.15.0 (The R Foundation for Statistical Computing). Bartlett's test was used to check the homogeneity of variance, one way ANOVA was carried out and Tukey test was used to determine statistically significant differences among means ( $p < 0.05$ ).

### 3. Results and discussion

#### 3.1. Individual vs combined US-HPH nanoemulsification preliminary trials

Preliminary trials were performed to assess the capability of US-HPH combined processes to produce nanoemulsions containing 2% (w/w) Tween 80 or whey protein isolate, as emulsifiers, in comparison to US and HPH individual treatments. In particular, the combined US-HPH processes consisted of 20 s or 60 s US followed by HPH process at 20, 50, 80 and 100 MPa. The reverse process (HPH-US) was not considered based on previous results highlighting that only US before HPH allowed the efficacy of combined process to be improved (Calligaris et al., 2016). The individual US treatments were conducted for 20 to 240 s, whereas HPH homogenization was performed by increasing pressure from 20 to 150 MPa for 1 pass, and at 120 MPa for 3 passes. The energy densities provided by the combined treatments to the samples ranged from 20 to 360 MJ/m<sup>3</sup> (Table 2). Figure 1 shows the particle size distributions of emulsions stabilized by Tween 80 or whey protein isolate obtained by means of the combined US-HPH as well as single US and HPH processes.

US-HPH processes allowed obtaining monomodal distributions using both emulsifiers at US times and pressure levels as low as 20 s and 50 MPa, respectively (Figures 1a and 1b). It must be noted that monomodal distributions were also obtained in both Tween 80 and whey protein isolate stabilized emulsions by means of 240 s US (278 MJ/m<sup>3</sup>) and HPH at pressure higher than 80 MPa (80 MJ/m<sup>3</sup>) (Figures 1c, 1d, 1e and 1f). The particle distribution amplitude and the mean particle diameter decreased with the increase in the energy density provided to samples, as well evidenced by the distribution width, the mean particle diameter value and the corresponding polydispersity index (PDI) (Figure 1, Table 2). In the energy density range of 78-125 MJ/m<sup>3</sup>, particles with diameter of about 220 nm and 300 nm were obtained using Tween 80 and whey protein isolate, respectively (Table 2). Combined treatments at energies of 155-175 MJ/m<sup>3</sup> further reduced the distribution width and particle dimensions below 220 nm (Figure 1, Table 2). It is noteworthy that diameters in the same order of magnitude were obtained only by applying 3 passes HPH at 120 MPa, corresponding 360 MJ/m<sup>3</sup> of energy density (Table 2). Such high energy levels pose different issues, including rapid wear and tear of plants and high energy consumption, which, in turn, increase process costs and reduce process sustainability and industrial feasibility (Yang, Marshall-Breton, Leser, Sher, & McClements, 2012). By contrast, results of the study showed that the combination of US and HPH actually led to produce Tween 80 and whey protein isolate stabilized nanoemulsions at energy densities lower than those required by the individual treatments. Synergistic homogenization effects of US and HPH have been previously attributed to the effect of the sequential application of different emulsification processes (Calligaris et al., 2016). In particular,

the first homogenization by US would reduce particle dimension and distribution width of the coarse emulsion favouring the further droplet break-up in the second HPH step (Abbas et al., 2013; Calligaris et al., 2016; Pandolfe, 1995). Results of this study also shows that within each emulsifying process, the distribution width and the mean particle diameter of Tween 80 containing emulsions was lower than that of whey protein isolate containing ones (Figure 1, Table 2). This can be attributed to the chemical features of the considered emulsifiers and their ability to adsorb on oil-water interfaces. Being Tween 80 a small non-ionic surfactant, it can rapidly adsorb to the oil-water interface during high-energy emulsification leading to the formation of small particles (Amani, York, Chrystyn, & Clark, 2009; Ghosh, Mukherjee, & Chandrasekaran, 2013). On the contrary, due to their high molecular weight, globular whey proteins are expected to slowly cover oil droplet surface generated during the high-energy emulsification process (Adjonu, Doran, Torley, & Agboola, 2014; Dissanayake & Vasiljevic, 2009; O'Regan & Mulvihill, 2010; Pearce & Kinsella, 1978).

### 3.2. Identification of the best US-HPH emulsifying conditions

To define the best performing process conditions to obtain nanoemulsions at the lowest energy level, a three factors face centred central composite design (CCF) was used. To this aim, the oil content, emulsifier concentration and emulsification energy density were considered as independent variables and their effect on emulsion mean particle diameter was studied (Table 1). According to the results of the preliminary trials, US-HPH treatments were applied to provide samples with low-medium energy densities. Table 1 also shows the mean particle diameter of emulsions obtained under the different CCF conditions. The regression coefficients and the relative analysis of variance of the polynomial models for the dependent variables are presented in Table 3.  $R^2_{adj}$  values for the responses were higher than 0.894.

The results showed that linear and quadratic terms of energy density ( $E_v$  and  $E_v^2$ , respectively), and linear terms of oil (*Oil*) and emulsifier (*Emuls*) contents had significant effects on mean particle diameter of Tween 80 stabilized emulsions, showing *p*-values lower than 0.001. Similarly, energy density (both linear and quadratic term) and oil content (linear term) significantly affected droplet dimensions of whey protein stabilized emulsions ( $p < 0.001$ , 0.01 and 0.05, respectively).

To evaluate the effects of the independent variables on the dependent one and to predict the optimum values of each variable for minimum mean droplet diameter to be achieved, contour-plots were generated. Figure 2 shows the contour-plots relevant to the effect of energy density and oil content (Figure 2a) or surfactant content (Figure 2b) on particle dimensions of Tween 80 stabilized emulsions. Nanoemulsions with the lowest diameter were obtained at the highest energy densities

and were associated to the lowest oil content (Figure 2a). In particular, the mean particle diameter decreased from about 400 nm to less than 160 nm as the energy density of the treatment increased. This indicated that the progressive enhancement of disruptive forces at the homogenization valve led to the generation of particles getting smaller due to the rapid absorption of Tween 80 at the oil/water interface. As the oil content increased at constant emulsifier level, the mean particle diameter also increased. It is likely that the passage at the homogenization valve of a higher quantity of oil reduced the efficacy of the treatment being the energy delivered to be shared between an increased oil quantity at a constant emulsifier concentration. Moreover, the surfactant content (2 % w/w) could be not enough to surround all the newly formed oil droplets. This observation is supported by results reported in Figure 2b, showing the mean particle diameter of Tween 80 stabilised emulsions as a function of energy density and emulsifier content, while maintaining oil content constant at 15 % (w/w). In fact, increasing the Tween 80 level produced a significant decrease in oil droplet dimensions.

Different behaviour was observed for whey protein stabilized emulsions (Figure 3). The minimum oil droplet diameter was achieved by transferring to the 10% (w/w) oil emulsion intermediate energies of about 110-140 MJ/m<sup>3</sup> (Figure 3a). Beyond these energy values, a further decrease of droplet size was not observed. Similar considerations can be also drawn by observing the plot of mean droplet diameter as a function of whey protein content and energy density (Figure 3b), by imposing 15% (w/w) value to the oil content variable. Also in this case, the best performing conditions in terms of emulsion droplet size were achieved at intermediate energy densities. It is possible that higher energy density values produced a progressive unfolding of whey proteins, leading to a reduction of their emulsifying properties. To this regard, different studies highlighted the capability of HPH to modify the protein structure. In particular, Oboroceanu et al. (2011) showed that high pressure microfluidization treatments (>50 MPa) of  $\beta$ -lactoglobulin induced 30% protein denaturation, accompanied by changes in secondary structure. Similarly, Bouaouina, Desrumaux, Loisel and Legrand (2006) reported that high pressure homogenization could modify the structure of whey protein, exposing the buried hydrophobic residues. Moreover, a recent study of Ali et al. (2018) reported HPH treatments to induced secondary structure transformation and protein aggregation via intermolecular disulfide bridges. Additionally, observing Figure 3b, it can be noted that whey protein isolate concentration did not to significantly affect the particle dimensions. An amount of 1% (w/w) whey proteins resulted to be sufficient to stabilize oil-water interface developed by the applied US-HPH combined treatments. Exceeding 1% (w/w) content, proteins were likely to locate in the continuous aqueous phase rather than at the oil-water interface

(Yan, Park, & Balasubramaniam, 2017). Based on these considerations, whey protein content can be minimized while maintaining good emulsification efficacy.

In the light of these results, the energy density developed by US-HPH process and the formulation conditions allowing the minimum dimension of emulsion oil droplets to be obtained, were estimated. For Tween 80 stabilized emulsions, 3% (w/w) emulsifier concentration, 10% (w/w) oil content and at least 145 MJ/m<sup>3</sup> energy density would guarantee emulsions with droplet diameter of 140-190 nm. In the case of whey protein stabilized emulsions, a minimum droplet size around 200-250 nm can be achieved by supplying energy density values lower than 120 MJ/m<sup>3</sup> to an emulsion containing 10% (w/w) oil and 1% (w/w) emulsifier.

### 3.3. *Effect of energy density share between US and HPH during combined emulsification processes*

Different combinations of US time and HPH pressure can be employed to deliver the same energy density during a US-HPH process. For instance, 120 MJ/m<sup>3</sup> can be transferred to the system by applying 22 s+90 MPa, 44 s+60 MPa or 75 s+30 MPa. Therefore, the last part of the research aimed to study the effect of the ratio between US and HPH in delivering the energy density during US-HPH nanoemulsification. The total energy densities, oil and emulsifier contents were selected based on CCF results as those allowing the lowest nanoemulsion droplet diameter to be generated. Energy density, oil content and emulsifier concentrations were 145 MJ/m<sup>3</sup>, 10% (w/w) and 3% (w/w) for the Tween 80 containing system; 120 MJ/m<sup>3</sup>, 10% (w/w) and 1% (w/w) for whey protein isolate containing one. The selected energy densities were, then, provided by using different combinations of US time and HPH pressure, progressively increasing the energy share generated by US and concomitantly reducing the one delivered by HPH, as shown in Table 4.

All combined processes resulted in lower particle dimensions than the corresponding individual homogenization treatments delivering the same energy density, in agreement with the CCF data and previously reported results (Calligaris et al., 2016). In particular, in the case of Tween 80 containing emulsions, the combinations in which 50-75% of the total energy density was delivered by HPH and the remaining energy by US, resulted in particle diameters in the range of 150-170 nm. It is noteworthy that an increase in energy share delivered by US (75%), with a concomitant reduction of HPH-delivered one (25%), produced larger diameters, confirming the higher emulsification efficacy of HPH as compared to US. Similarly, in the case of whey protein isolate stabilized emulsions, lower diameters were observed when at least 50% of total energy share was delivered by HPH. These treatments, in fact, allowed particles with mean diameters of about 230 nm to be obtained, again validating the CCF model. It can be concluded that the high pressure homogenization step of

the combined process has to be considered the critical phase to obtain fine emulsions. The US treatment before HPH would prevalently serve to reduce particle size and distribution width of the coarse emulsion before entering in the homogenization valve. In other words, the US step would improve the efficiency of the second HPH homogenization in obtaining particles even lower.

## Conclusions

In this work, the efficacy of combined US-HPH emulsification processes at low energy density to obtain nanoemulsions was demonstrated. Moreover, the proposed combined nanoemulsification appears to be versatile, since it can be exploited by using different levels of both Tween 80 and whey protein isolate as emulsifiers as well as oil at different contents. Depending on the emulsifier used in the formulation, the best performing processing parameters (total energy density and energy density share between US and HPH) and formulation conditions (oil and emulsifier contents) has to be tested and defined. In fact, the emulsifier characteristics greatly affected the performances of combined US-HPH process. In all cases, the combined process led to nanoemulsions at energy density levels which were approximately half of those required by single US or HPH to obtain the same emulsification performances in terms of mean particle diameter.

From an industrial perspective, these results open interesting possible opportunities in the attempt to design more sustainable emulsification processes and devices. It should be stressed that homogenization pressure lower than 60 MPa and ultrasonication duration of a few seconds appear compatible with the actual industrial needs, leading to a possible reduction of the total ownership cost. Finally, the proposed approach could definitively contribute to increasing the exploitability of nanoemulsions in food at large-scale production facilities.

## Acknowledgements

Authors are grateful to Dr. Annalisa Malchiodi and Dr. Silvia Grasselli of Gea Mechanical Equipment Italia for technical support in HPH processing and to Dr. Federica Sfiligoi for contributing to analyses.

## References

- Abbas, S., Hayat, K., Karangwa, E., Bashari, M., & Zhang, X. (2013). An overview of ultrasound-assisted food-grade nanoemulsions. *Food Engineering Reviews*, 5, 139-157.
- Adjonu, R., Doran, G., Torley, P., & Agboola, S. (2014). Formation of whey protein isolate hydrolysate stabilised nanoemulsion. *Food Hydrocolloids*, 41, 169-177.
- Ali, A., Le Potier, I., Huang, N., Rosilio, V., Cheron, M., Faivre, V., ... , & Mekhloufi, G. (2018).

- Effect of high pressure homogenization on the structure and the interfacial and emulsifying properties of Beta-Lactoglobulin. *International Journal of Pharmaceutics*, 537, 111-121.
- Amani, A., York, P., Chrystyn, H., & Clark, B. J. (2009). Factors affecting the stability of nanoemulsions-Use of artificial neural networks. *Pharmaceutical Research*, 27, 37.
- Bot, F., Calligaris, S., Cortella, G., Plazzotta, S., Nocera, F., & Anese, M. (2017). Study on high pressure homogenization and high power ultrasound effectiveness in inhibiting polyphenoloxidase activity in apple juice. *Journal of Food Engineering*, <https://doi.org/10.1016/j.jfoodeng.2017.10.009>.
- Bouaouina, H., Desrumaux A., Loisel, C., and Legrand, J. (2006). Functional properties of whey proteins as affected by dynamic high-pressure treatment. *International Dairy Journal*, 16, 275-84.
- Calligaris, S., Plazzotta, S., Bot, F., Grasselli, S., Malchiodi, A., & Anese, M. (2016). Nanoemulsion preparation by combining high pressure homogenization and high power ultrasound at low energy densities. *Food Research International*, 83, 25-30.
- Canselier, J. P., Delmas, H., Wilhelm, A. M., & Abismail, B. (2002). Ultrasound emulsification-An overview. *Journal of Dispersion Science and Technology*, 23, 333-349.
- Dissanayake, M., & Vasiljevic, T. (2009). Functional properties of whey proteins affected by heat treatment and hydrodynamic high-pressure shearing. *Journal of Dairy Science*, 92, 1387-1397.
- Dumay, E., Chevalier-Lucia, D., Picart-Palmade, L., Benzaria, A., Gràcia-Julià, A., & Blayo, C. (2013). Technological aspects and potential applications of (ultra) high-pressure homogenisation. *Trends in Food Science & Technology*, 31, 13-26.
- Ghosh, V., Mukherjee, A., & Chandrasekaran, N. (2013). Ultrasonic emulsification of food-grade nanoemulsion formulation and evaluation of its bactericidal activity. *Ultrasonics Sonochemistry*, 20, 338-344.
- Jafari, S. M., Assadpoor, E., He, Y., & Bhandari, B. (2008). Re-coalescence of emulsion droplets during high-energy emulsification. *Food Hydrocolloids*, 22, 1191-1202.
- Karthik, P., Ezhilarasi, P. N., & Anandharamakrishnan, C. (2017). Challenges associated in stability of food grade nanoemulsions. *Critical Reviews in Food Science and Nutrition*, 57, 1435-1450.
- Kentish, S., Wooster, T. J., Ashokkumar, M., Balachandran, S., Mawson, R., & Simons, L. (2008). The use of ultrasonics for nanoemulsion preparation. *Innovative Food Science & Emerging Technologies*, 9, 170-175.
- Leong, T. S. H., Wooster, T. J., Kentish, S. E., & Ashokkumar, M. (2009). Minimising oil droplet size using ultrasonic emulsification. *Ultrasonics Sonochemistry*, 16, 721-727.
- McClements, D. J., & Rao, J. (2011). Food-grade nanoemulsions: formulation, fabrication,

- properties, performance, biological fate and potential toxicity. *Critical Reviews in Food Science and Nutrition*, 51, 285-330.
- McClements, D.J. (2005). *Food Emulsions: Principle, Practice and Techniques* (2<sup>nd</sup> edition), Boca Raton, FL: CRC press.
- Mohd-Setapar, S. H., Nian-Yian, L., Nuraisha, W., Kamarudin, W., & Idham, Z. (2013). Omega-3 emulsion of Rubber (*Hevea brasiliensis*) seed oil. *Agricultural Sciences*, 4, 84-89.
- O'Regan, J., & Mulvihill, D. M. (2010). Sodium caseinate-maltodextrin conjugate hydrolysates: Preparation, characterisation and some functional properties. *Food Chemistry*, 123, 21-31.
- Pandolfe, W. D. (1995). Effect of premix condition, surfactant concentration and oil level on the formation of oil-in-water emulsions by homogenization. *Journal of Dispersion Science and Technology*, 16, 633-650.
- Oboroceanu D., Wang L., Kroes-Nijboer A., Brodkorb A., P. Venema, Magner E., & Auty M. A. E. (2011). The effect of high pressure microfluidization on the structure and length distribution of whey protein fibrils. *International Dairy Journal*, 21, 823-830.
- Pearce, K. N., & Kinsella, J. E. (1978). Emulsifying properties of proteins: evaluation of a turbidimetric technique. *Journal of Agricultural and Food Chemistry*, 26, 716-723.
- Qian, C., & McClements, D. J. (2011). Formation of nanoemulsions stabilized by model food-grade emulsifiers using high-pressure homogenization: Factors affecting particle size. *Food Hydrocolloids*, 25, 1000-1008.
- Raso, J., Mañas, P., Pagán, R., & Sala, F. J. (1999). Influence of different factors on the output power transferred into medium by ultrasound. *Ultrasonics Sonochemistry*, 5, 157-162.
- Salvia-Trujillo, L., Soliva-Fortuny, R., Rojas-Grau, M. A., McClements, D. J., & Martin-Belloso, O. (2017). Edible nanoemulsions as carriers of active ingredients: a review. *Annual Review of Food Science and Technology*, 28, 439-466.
- Sanguansri, P., & Augustin, M. A. (2006). Nanoscale materials development-a food industry perspective. *Trends in Food Science & Technology*, 17, 547-556.
- Schubert, H., Ax, K., & Behrend, O. (2003). Product engineering of dispersed systems. *Trends in Food Science & Technology*, 14, 9-16.
- Schubert, H., & Engel, R. (2004). Product and formulation engineering of emulsions. *Chemical Engineering Research and Design*, 82, 1137-1143.
- Silva, H. D., Cerqueira, M. Â., & Vicente, A. A. (2012). Nanoemulsions for food applications: development and characterization. *Food and Bioprocess Technology*, 5, 854-867.
- Stang, M., Schuchmann, H., & Schubert, H. (2001). Emulsification in high-pressure homogenizers. *Engineering in Life Sciences*, 1, 151-157.



- Wooster, T. J., Golding, M., & Sanguansri, P. (2008). Impact of oil type on nanoemulsion formation and Ostwald ripening stability. *Langmuir*, 24, 12758-12765.
- Yan, B., Park, S. H., & Balasubramaniam, V. M. (2017). Influence of high pressure homogenization with and without lecithin on particle size and physicochemical properties of whey protein-based emulsions. *Jurnal of Food Process Engineering*, 40, 1-10.
- Yang, Y., Marshall-Breton, C., Leser, M. E., Sher, A. A., & McClements, D. J. (2012). Fabrication of ultrafine edible emulsions: Comparison of high-energy and low-energy homogenization methods. *Food Hydrocolloids*, 29, 398-406.

**Caption of Figures**

Figure 1. Particle dimension distributions of emulsions containing 2% Tween 80 (a, c, e) or whey proteins (b, d, f), produced by means of US-HPH (20 s + 20 MPa, 20 s + 50 MPa, 60 s + 50 MPa and 60 s + 100 MPa), US (20, 60, 120 and 240 s) and HPH (1 pass at 20, 80, 150 MPa and 3 passes at 120 MPa) treatments.

Figure 2. Fitted contour plots of mean particle diameter of Tween 80 stabilized emulsions as a function of energy density ( $E_v$ ) and oil content (Oil) (a) or emulsifier concentration (*Emuls*) (b). The value of the emulsifier concentration was kept at the central point (2% w/w).

Figure 3. Fitted contour plots of mean particle diameter of whey protein stabilized emulsions as a function of energy density ( $E_v$ ) and oil content (Oil) (a) or emulsifier concentration (*Emuls*) (b). The value of the oil content was kept at the central point (15% w/w).

Table 1. Combinations of oil content, emulsifier concentration and energy density of different runs and experimental results  $\pm$  standard deviation of a three factors face centred central composite design

Run	Oil (% w/w)	Emulsifier (% w/w)	Energy density (MJ/m <sup>3</sup> )	Mean particle diameter (nm)	
				Tween 80	Whey protein isolate
1	10	1	47	420 $\pm$ 43	344 $\pm$ 12
2	10	3	47	340 $\pm$ 34	353 $\pm$ 22
3	20	3	47	389 $\pm$ 6	411 $\pm$ 15
4	20	1	47	488 $\pm$ 59	427 $\pm$ 23
5	10	1	175	212 $\pm$ 11	257 $\pm$ 29
6	10	3	175	128 $\pm$ 13	239 $\pm$ 2
7	20	1	175	323 $\pm$ 18	285 $\pm$ 14
8	20	3	175	194 $\pm$ 8	241 $\pm$ 15
9	10	2	111	220 $\pm$ 10	233 $\pm$ 7
10	20	2	111	277 $\pm$ 9	279 $\pm$ 11
11	15	1	111	257 $\pm$ 21	285 $\pm$ 7
12	15	3	111	210 $\pm$ 11	228 $\pm$ 4
13	15	2	47	397 $\pm$ 46	463 $\pm$ 31
14	15	2	175	215 $\pm$ 7	240 $\pm$ 8
15	15	2	111	239 $\pm$ 13	287 $\pm$ 13
16	15	2	111	240 $\pm$ 11	279 $\pm$ 10
17	15	2	111	249 $\pm$ 21	296 $\pm$ 3
18	15	2	111	248 $\pm$ 9	279 $\pm$ 21
19	15	2	111	249 $\pm$ 12	293 $\pm$ 24
20	15	2	111	247 $\pm$ 12	215 $\pm$ 16

Table 2. Mean particle diameter and polydispersity index (PDI) ( $\pm$  standard deviation) of emulsions containing 2% (w/w) Tween 80 or whey protein isolate, subjected to HPH and US provided in combination or individually at increasing energy density.

Treatment	Pressure (MPa)	Passes	Time (s)	Energy density (MJ/m <sup>3</sup> )	Tween 80		Whey proteins	
					Mean particle diameter (nm)	PDI	Mean particle diameter (nm)	PDI
US-HPH	20		20	41	296 $\pm$ 12 <sup>c</sup>	0.35 $\pm$ 0.07 <sup>cde</sup>	430 $\pm$ 9 <sup>b</sup>	0.54 $\pm$ 0.08 <sup>b</sup>
	50		20	78	221 $\pm$ 9 <sup>ef</sup>	0.24 $\pm$ 0.04 <sup>de</sup>	291 $\pm$ 3 <sup>cd</sup>	0.37 $\pm$ 0.01 <sup>bcd</sup>
	80		20	108	208 $\pm$ 11 <sup>fgh</sup>	0.28 $\pm$ 0.00 <sup>de</sup>	304 $\pm$ 10 <sup>bc</sup>	0.33 $\pm$ 0.01 <sup>bcd</sup>
	50		60	125	225 $\pm$ 12 <sup>ef</sup>	0.25 $\pm$ 0.01 <sup>de</sup>	280 $\pm$ 8 <sup>de</sup>	0.35 $\pm$ 0.09 <sup>bcd</sup>
	80		60	155	194 $\pm$ 10 <sup>hi</sup>	0.22 $\pm$ 0.03 <sup>ef</sup>	218 $\pm$ 1 <sup>fg</sup>	0.21 $\pm$ 0.05 <sup>fg</sup>
	100		60	175	190 $\pm$ 1 <sup>hi</sup>	0.17 $\pm$ 0.01 <sup>f</sup>	205 $\pm$ 5 <sup>fg</sup>	0.17 $\pm$ 0.01 <sup>g</sup>
US			20	21	475 $\pm$ 21 <sup>a</sup>	0.69 $\pm$ 0.04 <sup>a</sup>	Phase separation	
			60	75	361 $\pm$ 22 <sup>b</sup>	0.49 $\pm$ 0.02 <sup>b</sup>	498 $\pm$ 4 <sup>a</sup>	0.75 $\pm$ 0.01 <sup>a</sup>
			120	143	385 $\pm$ 10 <sup>b</sup>	0.49 $\pm$ 0.03 <sup>b</sup>	441 $\pm$ 17 <sup>ab</sup>	0.47 $\pm$ 0.01 <sup>bc</sup>
			240	278	258 $\pm$ 2 <sup>cd</sup>	0.38 $\pm$ 0.04 <sup>bc</sup>	299 $\pm$ 13 <sup>bc</sup>	0.42 $\pm$ 0.03 <sup>bc</sup>
HPH	20	1		20	363 $\pm$ 8 <sup>b</sup>	0.41 $\pm$ 0.02 <sup>cd</sup>	389 $\pm$ 15 <sup>b</sup>	0.43 $\pm$ 0.01 <sup>bc</sup>
	50	1		50	265 $\pm$ 12 <sup>cd</sup>	0.34 $\pm$ 0.08 <sup>cde</sup>	292 $\pm$ 13 <sup>cd</sup>	0.30 $\pm$ 0.03 <sup>cd</sup>
	80	1		80	228 $\pm$ 6 <sup>ef</sup>	0.27 $\pm$ 0.01 <sup>de</sup>	250 $\pm$ 14 <sup>ef</sup>	0.27 $\pm$ 0.03 <sup>ef</sup>
	120	1		120	229 $\pm$ 16 <sup>ef</sup>	0.26 $\pm$ 0.06 <sup>de</sup>	243 $\pm$ 7 <sup>ef</sup>	0.27 $\pm$ 0.04 <sup>ef</sup>
	150	1		150	208 $\pm$ 6 <sup>fgh</sup>	0.23 $\pm$ 0.02 <sup>ef</sup>	245 $\pm$ 13 <sup>ef</sup>	0.27 $\pm$ 0.03 <sup>ef</sup>
	120	3		360	168 $\pm$ 2 <sup>i</sup>	0.15 $\pm$ 0.01 <sup>f</sup>	182 $\pm$ 4 <sup>g</sup>	0.16 $\pm$ 0.03 <sup>g</sup>

<sup>a-i</sup>: within each column, means with different letters are statistically different (p<0.05)

Table 3. Regression coefficients of the models for mean particle diameter of emulsions stabilized with Tween 80 and whey proteins

Variable	Tween 80	Whey proteins
Intercept	637.167	261.447
$E_v$	-5.697 ***	-4.881 ***
$E_v^2$	0.018 ***	0.021 **
Oil	-2.880 ***	32.172 *
Oil <sup>2</sup>	0.348	-0.680
Emuls	15.212 ***	83.995
Emuls <sup>2</sup>	-6.873	-16.408
$E_v \times \text{Oil}$	0.024	-0.044
$E_v \times \text{Emuls}$	-0.070	-0.104
Oil x Emuls	-1.594	-1.297
$R^2_{\text{adj}}$	0.981	0.894

\* :  $p < 0.05$ ; \*\* :  $p < 0.01$ ; \*\*\* :  $p < 0.001$

Table 4. Mean particle diameter obtained by the application of different combined US-HPH processes delivering energy densities of 145 and 120 MJ/m<sup>3</sup> to systems containing Tween 80 and whey protein isolate, respectively.

Emulsifier	US time (s)	HPH pressure (MPa)	Total energy density (MJ/m <sup>3</sup> )	Energy delivered by US (%)	Energy delivered by HPH (%)	Mean particle diameter (nm)
Tween 80	0	145	145	0	100	278 ± 7 <sup>b</sup>
	26	109		25	75	170 ± 9 <sup>de</sup>
	50	73		50	50	151 ± 8 <sup>e</sup>
	90	36		75	25	196 ± 3 <sup>c</sup>
	100	0		100	0	389 ± 7 <sup>a</sup>
Whey proteins	0	120	120	0	100	342 ± 10 <sup>b</sup>
	22	90		25	75	228 ± 6 <sup>d</sup>
	41	60		50	50	231 ± 5 <sup>d</sup>
	75	30		75	25	270 ± 4 <sup>c</sup>
	81	0		100	0	386 ± 4 <sup>a</sup>

<sup>a-c</sup>: in the same emulsifier group, means with different letters are statistically different (p<0.05)

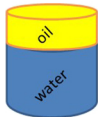
**Highlights**

Combined US-HPH process allowed obtaining nanoemulsions using food grade emulsifiers

US-HPH process allowed nanoemulsification energy density to be reduced

Oil and emulsifier content and energy density affected US-HPH emulsification efficacy

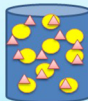
US and HPH energy levels affected US-HPH nanoemulsification performance



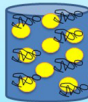
Nanoemulsification by combining  
**US + HPH**  
at low-medium energy density

US = high-power ultrasound  
HPH = high-pressure homogenization

NANOEMULSION  
with  $\varnothing < 200$  nm



Tween80



Whey proteins

Graphics Abstract



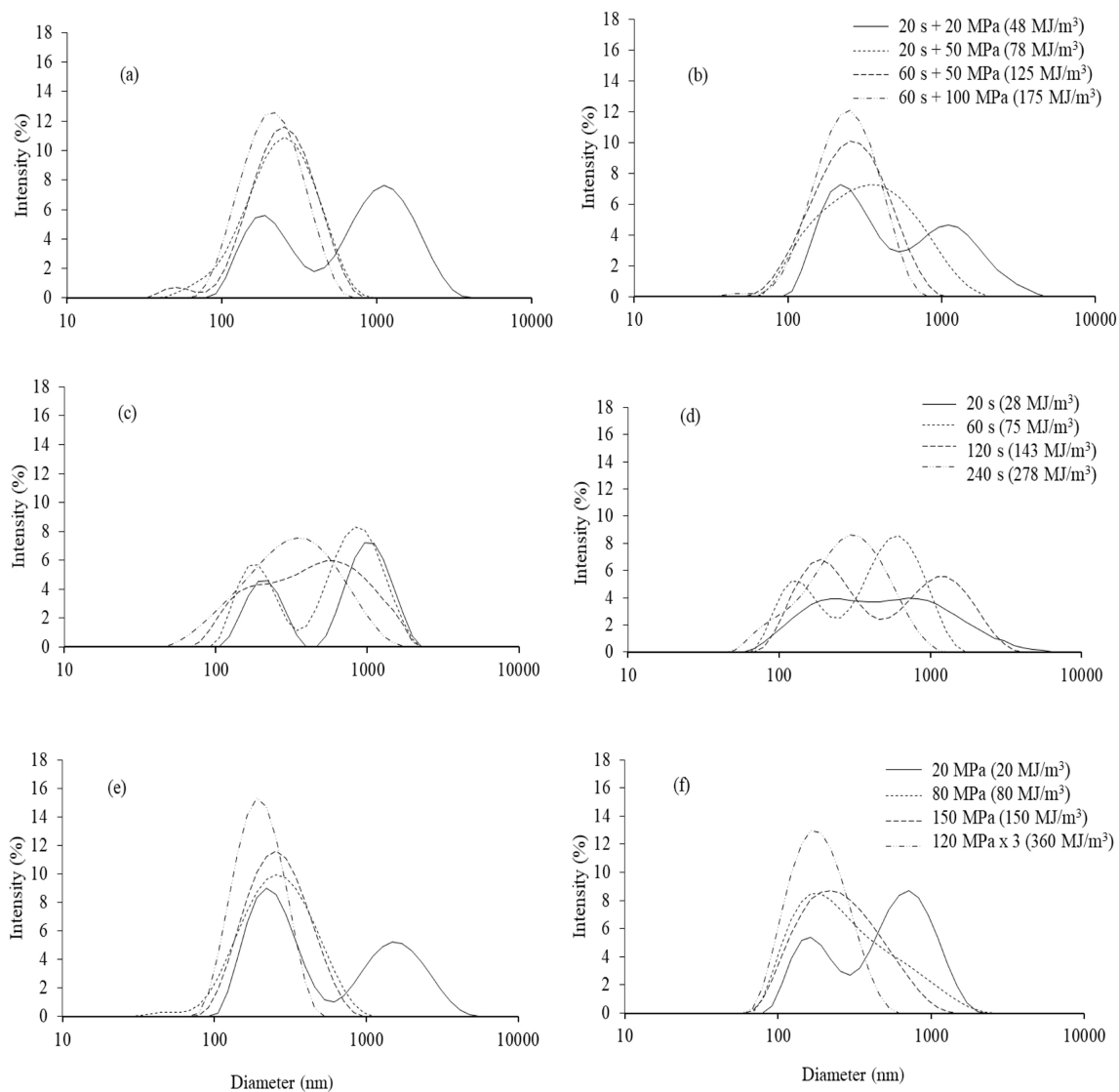


Figure 1

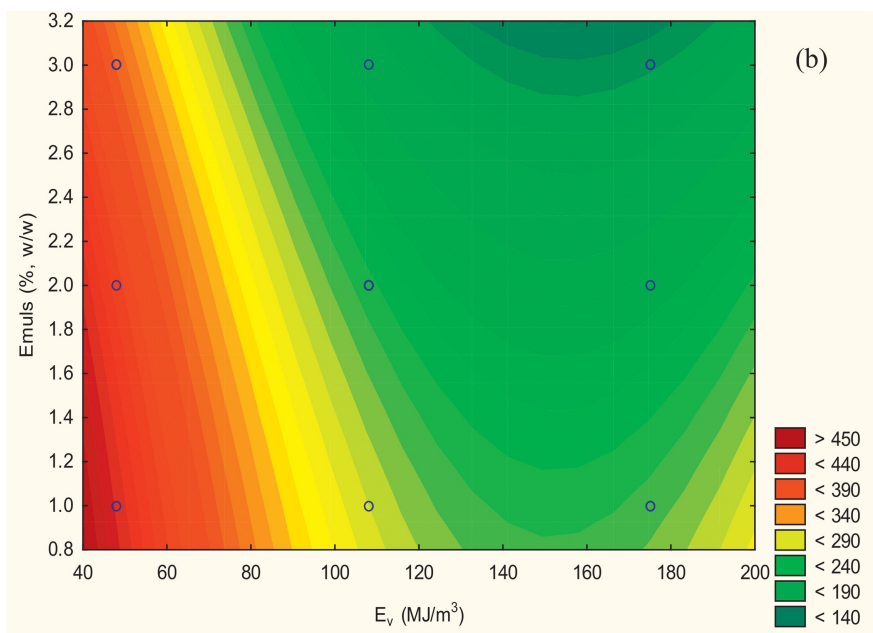
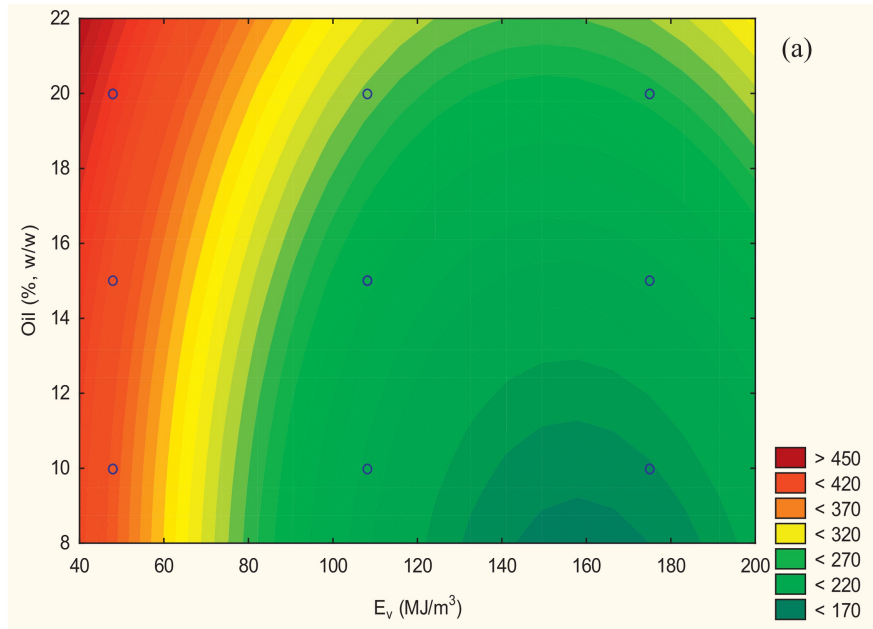


Figure 2

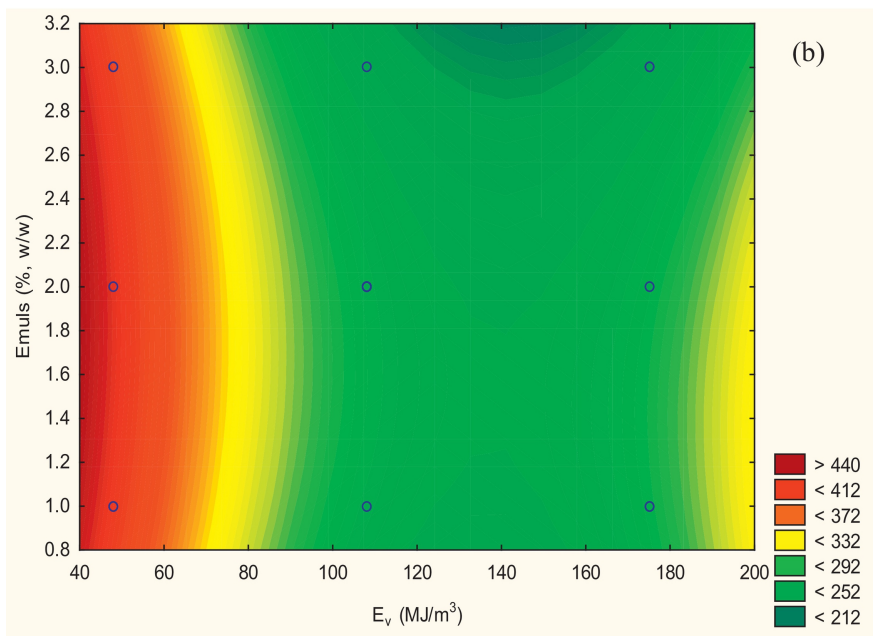
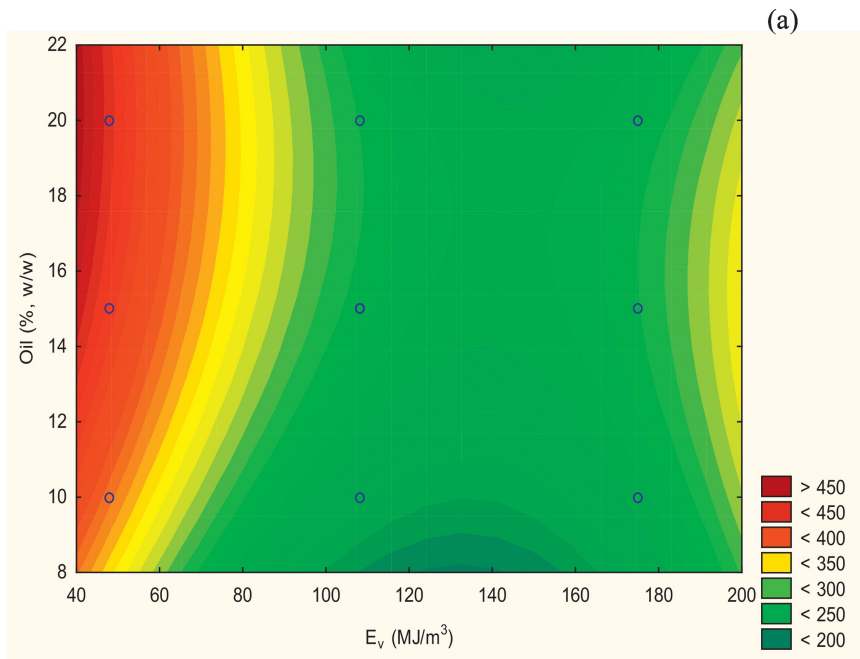


Figure 3